ADVANCED FUNCTIONAL MATERIALS
www.afm-journal.de

Fungal Innovation: Harnessing Mushrooms for Production of Sustainable Functional Materials

Anne Zhao, Linn Berglund, Luísa Rosenstock Völtz, Renald Swamy, Io Antonopoulou, Shaojun Xiong, Johanne Mouzon, Alexander Bismarck,* and Kristiina Oksman**

Underutilized co- and by-products are upgraded into materials with functional properties. The utilization of mushroom farming residues is investigated, specifically mushroom residues and spent mushroom substrate – whose chemical composition is determined – to produce cosmetic face masks, packaging films, and oil sorbents. Flexible mushroom sheets exhibit conformability and antioxidant activity between 82 and 94%, and better tensile strength in comparison with commercial cosmetic masks, making them suitable for such applications. Plasticization with glycerol increases the flexibility and tensile strain from ≈1 to 45% and moisture sorption from 32 to 100 wt.%. Spent mushroom substrate pulp yields stiff and strong rigid sheets with Young's moduli of 5 GPa and tensile strengths of 42 MPa. These sheets show 100% antioxidant activity, having hydrophobic behavior and oxygen barrier properties in dry conditions, and thus are promising for bioactive packaging applications. Foamed spent mushroom substrate sorbents demonstrate high affinity for both oil and water, with a water and oil uptake of 21 and 28 times their weight, respectively, while maintaining structural integrity. These properties make the foams viable as bio-based oil sorbents, highlighting the potential of by-products for advanced functional materials.

1. Introduction

The global mushroom and truffle production in 2021 was 44.2 million tonnes,[1] which was valued at US$ 50.3 billion and is predicted to grow at a compound annual growth rate of 9.7% until 2030.[2] Fungi and mushrooms are increasingly used to produce processed meat replacement products,[3,4] whose market share is growing driven by changing dietary habits. Edible mushroom production generates significant amounts of fruiting body residues; up to 20% of the total mushrooms are discarded because of misshaped caps or stalks.[5] The base and stems of mushrooms make up 25–33 wt% of fresh mushrooms and are often disposed of because of their tough texture.[6] Discarded mushrooms, which fail to meet the commercial standard of retailers along with leftover stems after harvest, are termed "mushroom residue" (MR). Edible mushrooms are grown on

A. Zhao, A. Bismarck
Polymer & Composite Engineering (PaCE) Group
Institute of Materials Chemistry & Research
Faculty of Chemistry
University of Vienna
Vienna A-1090, Austria
E-mail: alexander.bismarck@univie.ac.at

L. Berglund, L. Rosenstock Völtz, R. Swamy, J. Mouzon, A. Bismarck, K. Oksman
Division of Materials Science
Department of Engineering Sciences and Mathematics
Luleå University of Technology
Luleå SE-971 87, Sweden
E-mail: linn.berglund@ltu.se; kristiina.oksman@ltu.se

L. Rosenstock Völtz, R. Swamy, K. Oksman
WWSC Wallenberg Wood Science Center
Luleå University of Technology
Luleå SE-971 87, Sweden

The ORCID identification number(s) for the author(s) of this article can be found under https://doi.org/10.1002/adfm.202412753

DOI: 10.1002/adfm.202412753

I. Antonopoulou
Department of Civil, Environmental and Natural Resources Engineering
Luleå University of Technology
Luleå SE-97 187, Sweden

S. Xiong
Department of Forest Biomaterial and Technology
Swedish University of Agricultural Sciences
Umeå SE-901 83, Sweden

A. Bismarck
Department of Chemical Engineering
Imperial College London
London SW7 2AZ, UK

A. Bismarck, K. Oksman
WISE Wallenberg Initiative for Sustainable Materials
Luleå University of Technology
Luleå SE-971 87, Sweden

K. Oksman
Department of Mechanical & Industrial Engineering (MIE) University of Toronto
Toronto M5S 3G8, Canada

substrates consisting of lignocellulosic biomass, typically wood particles supplemented with small amounts of nutrients. Once the mushrooms are harvested, the remaining substrate is termed "spent mushroom substrate" (SMS). Considering the scale of commercial mushroom production, typically 5 kg of substrate yields 1 kg of fresh mushrooms/fruiting bodies, resulting in massive amounts of spent mushroom substrate.[7] Taking the data reported by U.N. Faostat [1] of the production volume of mushrooms ≈104 million tonnes SMS was generated in 2011 and this grew to ≈221 million tonnes in 2021, and is expected to grow further with increasing demand. Given the substantial quantities of under-utilized MR and SMS, it is crucial to explore innovative valorization pathways. We will explore various research approaches aiming to transform the mushroom-farming by-products and residues into value-added products and introduce novel applications for both MR and SMS.

1.1. Mushroom Residue and Its Use

Fungi-derived materials have received significant interest for various applications, including textiles,[8] paper,[9] and filters for water treatment[10,11] due to their unique mechanical properties and sustainability. Engineered living self-healing materials can be produced utilizing living fungal cells.[12] Besides materials, mushroom residues (MR) were also repurposed into antioxidative compounds such as vitamin D2,[5] finding use in the food and pharmaceutical industry. Other potential applications of MR in the food sector include enhancing the texture and shelf life of food products.[13] Carbonized MR can serve as electrodes in electrochemical energy storage systems.[14,15] Fungi are a source of chitin – a rigid polysaccharide comprising N-acetyl-D-glucosamine units linked by (1,4)-β-glycosidic bonds – serving as the key structural element in fungal cell walls and exoskeletons of arthropods, such as insects and crustaceans.[16] Within fungi, chitin appears as nanofibrils, deriving its strength primarily from hydrogen bonds between macromolecular chains.[16] Unlike crustacean chitin, fungal-derived chitin is covalently linked to β-glucan, another structural element in the fungal cell wall composed of glucose units mainly linked by linear (1,3)-β-glycosidic bonds.[17] The chitin-β-glucan complex constitutes a natural composite combining the strength of chitin with the flexibility and toughness of β-glucan, enhancing film-forming properties.[9] Nawawi et al.[18] demonstrated the potential to use common mushrooms to manufacture chitin-glucan films with outstanding mechanical properties. They isolated chitin-glucan from fungal biomass by blending *Agaricus bisporus* (white button mushroom) using extraction in distilled water followed by 1 M NaOH.[18] The properties of chitin-glucan films can be tuned by varying the β-glucan content, achieved by adding *Daedaleopsis confragosa* (tree bracket fungi), which are rich in β-glucan.[19] Bilbao-Sainz et al.[20] further highlighted the valorization of discarded white button mushroom stems for biodegradable chitosan films. Sun et al.[21] reported multi-functional chitin-glucan sponges with shape-memory for the application as hemostatic agents, by partially removing proteins and glucan from *Pleurotus eryngii* fruiting bodies through alkali treatment and TEMPO oxidation followed by crosslinking. The increased interest in fungal material innovations prompted us to explore further novel applications. The optimization of MR sheets disclosed by Nawawi et al.[18] presents an innovative opportunity to repurpose mushroom residue into fungal-based cosmetic sheet masks. Cosmetic sheet masks are becoming increasingly popular in skincare routines, particularly in Asia-Pacific markets.[22–24] Conventional sheet masks – typically cotton or synthetic fiber-based single-use products – raise environmental concerns due to resource-intensive production and/or non-biodegradability.[23,25,26] Chitin, chitosan, and β-glucan have been increasingly used in cosmetic products due to their anti-microbial,[27] anti-oxidative,[28,29] and anti-inflammatory properties.[30,31] Besides chitin, fungal biomass contains numerous valuable components beneficial for skin health,[22] possessing anti-aging and moisturizing properties.[28] We extracted chitin-glucan complex from *A. bisporus* (white button) and *H. erinaceus* (lion's mane), using two different extraction methods with distilled water and 0.1 M NaOH, before turning the pulp into sheets whose properties were evaluated for cosmetic applications.

1.2. Spent Mushroom Substrate and Its Use

Besides mushroom residue, the next challenge to address is the valorization of the remaining spent mushroom substrate. SMS mainly consists of wood particle residues such as sawdust mainly composed of cellulose, hemicellulose, and lignin with fewer amounts of nutrients such as wheat bran and grains along with fungal mycelium.[32,33] During fungal cultivation, the mushroom forms a rootlike structure called mycelium and selective degradation of lignin occurs simultaneously, reducing its content up to 77% in comparison to the initial raw substrate.[32] Commonly, SMS has been used for relatively low value-added products, such as bioenergy production,[32,33] soil enhancement,[34,35] and animal feed.[36] Mycelium has also been explored for more advanced applications, one example is water purification filters for the removal of microplastic pollution.[11] Other examples are mycelium-composites in which mycelium acts as a binder for biomass.[37–39] One commercially available example of this is provided by GROWNBio who produce novel light-weight packaging and building materials with specific shapes.[40] The GROWNBio products also possess interesting functionalities such as fire-retardancy, and sound insulation, as well as a low carbon footprint. Recently, Attias et al.[41] reported a process they referred to as bio fabrication where hybrid materials of cellulose nanofiber-mycelium were produced by incubation of a mycelium culture in nutrient-rich liquid media to produce films proposed for packaging, filtration, and hygiene products. These products, however, are not making direct use of SMS as a by-product. For example, Konno et al.[42] used TEMPO-mediated oxidation of shitake SMS to produce cellulose nanofibers with a yield of 18% displaying typical nanofiber dimensions and properties. Li et al.[35] prepared chitin/cellulose nanofibers with a yield of 25% using SMS from shiitake cultivation as raw material targeting growth promotion and disease control of plants. Suksai et al.[43] used oyster and lingzhi mushroom SMS to produce natural fibers using a strong NaOH pretreatment followed by steam explosion. The addition of tapioca starch as a binder allowed to preparation of fiber sheets. The prepared sheets were suggested to be used for biodegradable

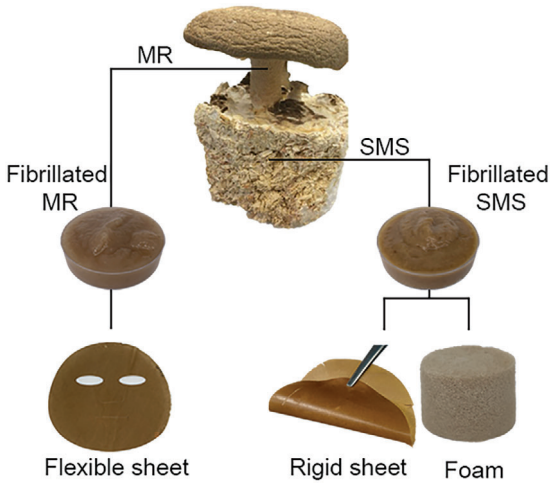

Scheme 1. A general overview of the concept for the development of advanced functional materials from by-products of the mushroom industry – mushroom residue (MR) and spent mushroom substrate (SMS), targeting cosmetics (flexible sheet), packaging (rigid sheet), and sorption (foam) applications. We demonstrated that by harnessing the natural characteristics of bioresources and using innovative technologies, advanced functional materials with specific properties for their intended applications can be developed.

packaging applications.[43] All previous studies either involved multiple processing steps with extensive use of chemicals or the addition of components for specific functionality. To date, very little research has been conducted on the use of SMS to prepare functional sustainable materials and even less on the utilization of the unique natural composition of SMS and the inherent functionalities they provide. In this work, SMS is fibrillated into pulp without chemical pretreatment using two different methods, and the pulps were processed into sheets and foams, and their properties were evaluated to propose novel applications.

1.3. Aims

We aim to transform MR and SMS, which are considered by-products, into novel functional green materials. We demonstrate how different mild extraction methods and fibrillation techniques can be applied to produce materials, such as flexible and rigid sheets for cosmetic face masks and packaging films/sheets as well as porous physical sorbents, with desired properties. The overall concept is visualized in the schematic below (**Scheme 1**). The functionalities of interest for the intended applications include mechanical and barrier properties, surface characteristics, water and oil sorption, and biodegradability.

2. Results and Discussions

2.1. Mushroom Residue and Spent Mushroom Substrate Materials

MR was mechanically fibrillated from fungal fruiting bodies of *Agaricus bisporus* (white button mushroom) and *Hericium erinaceus* (lion's mane mushroom) and the chitin-glucan complex was extracted using mild extraction methods, either with distilled water or with 0.1 M or 1 M NaOH, resulting in a brownish paste-like pulp, as shown in **Figure 1**a–c. The procedures using water or 0.1 M NaOH were adapted from Nawawi et al.[18] where a milder extraction process should preserve the natural composition, and bioactive components present in the raw material as much as possible. For comparison, *A. bisporus* pulp was also produced using the standard extraction method using 1 M NaOH following the procedure disclosed by Nawawi et al.[18] Figure 1a′–c′,a″–c″ show that fiber sizes and structure are similar irrespectively of the used extraction processes. All three extraction methods preserved the fungal microfilament (hyphae) structures, as demonstrated using optical light microscopy in Figure 1a′–c′ and scanning electron microscopy in Figure 1a″–c″. Figure 1c′ shows that MR pulp produced by water extraction contained hyphae still possessing internal cell components and spores, which were visible as dark patches in the SEM image in Figure 1c″. With increasing severity of NaOH extraction (0.1 to 1 M) increasing amounts of internal cell components and most spores were removed leaving empty cell walls only (Figure 1a′,b′). Water-swollen filament widths of MR pulp produced by 1 M NaOH extraction (9.1 ± 4.4 µm), 0.1 M NaOH extraction (13.2 ± 5.8 µm), and water extraction (9.5 ± 4.1 µm) were measured form optical micrographs and indicated similar sizes.

In contrast to MR, SMS was processed using different fibrillation techniques, without any chemical pretreatments to preserve its natural composition. SMS was disintegrated into pulp using ultrafine grinding (G) and co-rotating twin-screw extrusion (E), as presented in **Figure 2**.

After processing, the G-SMS pulp had a gel-like consistency while the E-SMS pulp had a dry fiber-like appearance, see Figure 2b,c. The "grainy" appearance of E-SMS was due to the high solids content of E-SMS (38 wt.%), while the solids content of G-SMS was much lower (6.5 wt.%) after the fibrillation process. Extrusion allows the processing of higher solid contents of the raw material compared with ultra-fine grinding. Optical microscopy and fiber size analysis were used to compare fiber size reduction; both methods reduced the original particle/fiber size, but ultrafine grinding (G) compared with extrusion (E) resulted in finer fibrils, although longer fibers were still present in both pulps (Figure 2b′,c′). This agreed with results from fiber size analysis (Table S1, Supporting Information) showing that 93% of G-SMS were below 0.2 mm, while 62% were within the same length fraction and only 28% were between 0.2–0.6 mm for E-SMS. Scanning electron micrographs of freeze-dried fibers showed a noticeable reduction in fiber size for both processed SMS materials compared to the original (Figure 2a′–a″). The micrographs of E-SMS show some intact wood fibers remaining after fibrillation, which was not observed for G-SMS. Mycelium appears to cover the fibers of both G- and E-SMS (Figure 2b″,c″). The viscosities of the pulps after fibrillation, measured at the same concentration of 6.5 wt.%, were determined to be 1490 ± 30 mPa s for G-SMS, compared to 110 ± 20 mPa s for E-SMS, signifying stronger network formation in G-SMS suspensions containing more separated fibrils. Comparing these two methods, extrusion is a more energy-efficient process, allowing more material to be fibrillated in a shorter time, while grinding results in finer fiber structures, as indicated by viscosity and microscopy.

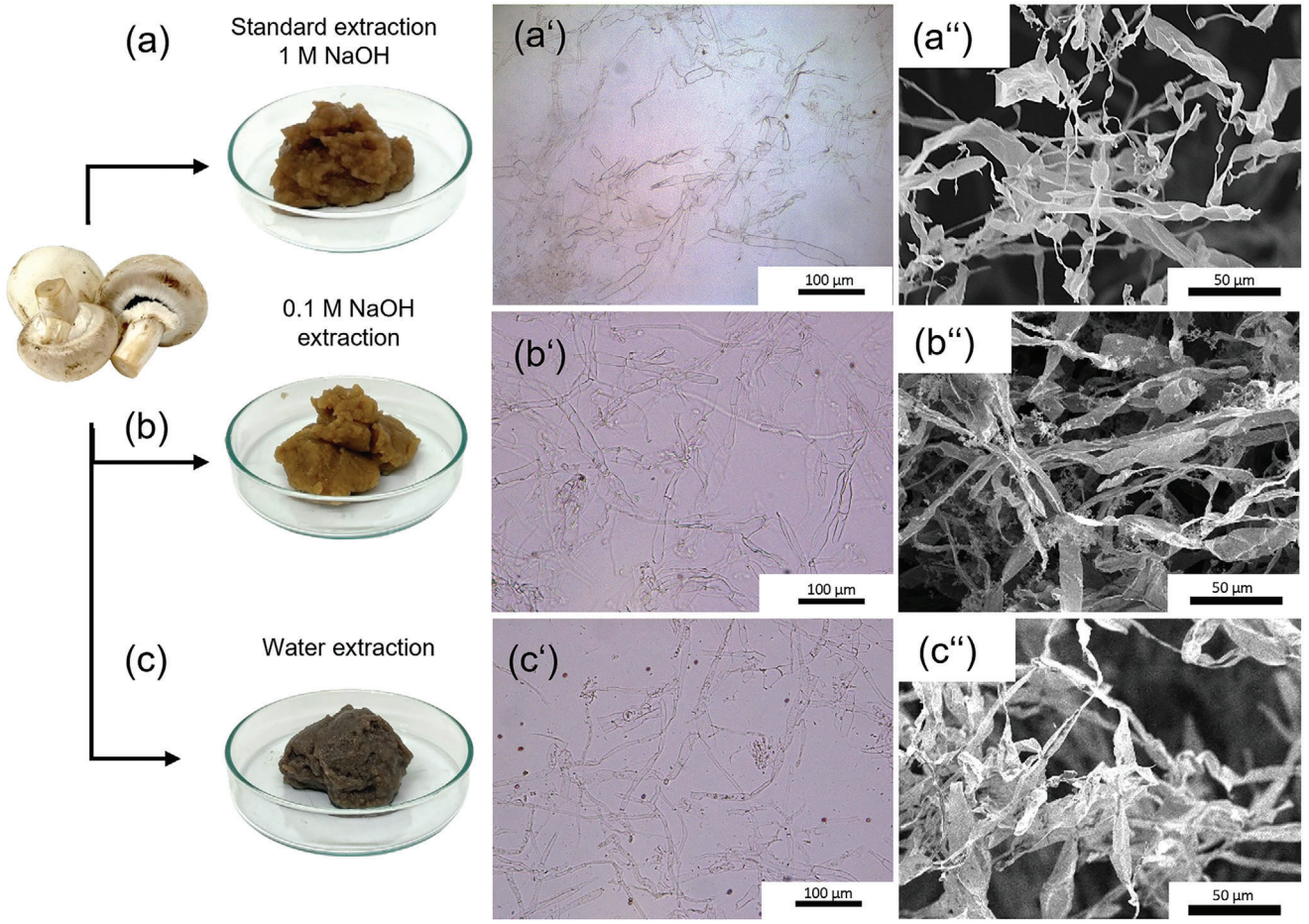

Figure 1. Overview of different parts of materials produced from mushroom residue (MR). MR pulp from *A. bisporus* was produced by the three extraction processes using a) 1 M NaOH, b) 0.1 M NaOH, and c) distilled water, (a′–c′) optical microscopy images and (a″–c″) scanning electron micrographs of dry pulp after the three processes, respectively. The width of water-swollen fungal hyphae was determined using ImageJ (n = 100).

The carbohydrate analysis and antioxidant activity, elemental analysis, and ssNMR of MR and SMS materials are presented in **Figure 3**. MR pulp produced by the standard method using 1 M NaOH contained 46% glucosamine associated with chitin/chitosan, while the MR pulp obtained using the milder extraction methods had a lower glucosamine content of 35% for extraction with 0.1 M NaOH and 24% for water-extracted MR pulp as shown in Figure 3a. The decreased glucosamine content was due to an increased amount of non-chitin-glucan components. The glucose content (34–28%) remained relatively constant irrespective of the extraction method used. The decreasing severity of the extraction medium (hot H_2O < 0.1 M NaOH < 1 M NaOH) resulted in a larger fraction of other alkali-soluble cell wall polysaccharides, such as α-glucan,[44] still being present in the fungal pulp. The fraction of non-polysaccharide components was larger for MR pulp produced by extraction with water (47%) and 0.1 M NaOH (29%) than for the original extraction method using 1 M NaOH (19%), demonstrating that milder extraction media preserved more cell walls components, such as proteins or antioxidative compounds like ergothioneine, vitamins, sterols, and phenolic compounds[45] leading to a higher radical scavenging activity. From Figure 3b, MR pulp displayed a radical scavenging activity of 94% after water extraction, compared to 82% after NaOH extraction at the highest concentration of material tested for 20 h of incubation. The elemental composition is shown in Figure 3c; all *A. bisporus* extracts remained relatively constant resembling reported values for *A. bisporus* biomass produced by extraction using 1 M NaOH.[46] Both MR pulps obtained by extraction from *H. erinaceus* contained considerably higher amounts of glucose (52% for 0.1 M NaOH extraction and 60% for water extraction) but less glucosamine (24% for 0.1 M NaOH extraction and 10% for water extraction, see Figure 3a) also reflected in the lower N content (Figure 3c) than extracts of *A. bisporus* indicating that less chitin/chitosan but higher amounts of polysaccharides comprising glucose were present in *H. erinaceus* than in *A. bisporus* pulp. Figure 3d shows the ssNMR spectra of all MR pulps. For MR pulp, the C1–C6 peaks between 55–103 ppm could be assigned to the glucose-backbone of chitin, chitosan, and β-glucan and signals for C═O at 173.5 ppm and –CH_3 at 22.5 ppm to chitin. The intensity of the ssNMR signals associated with chitin for MR pulp of *A. bisporus* decreased the milder the extraction method. Both pulps produced from *H. erinaceus* showed considerably lower C═O and ─CH_3 signals due to the lower glucosamine content.

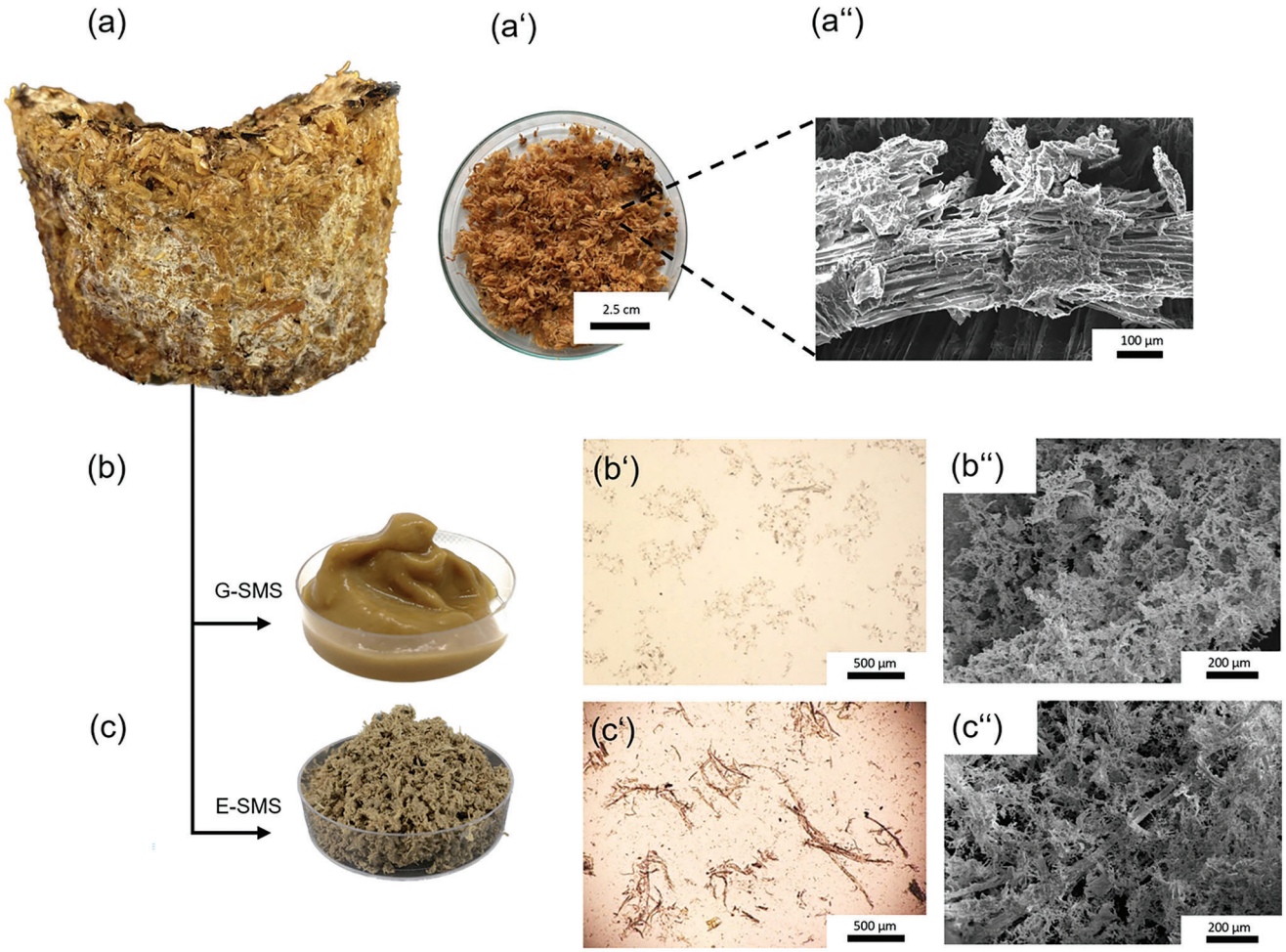

Figure 2. Overview of different parts of materials obtained from spent mushroom substrates (SMS). a) SMS, (a′) SMS after manual disintegration, and (a″) microstructure of a wood particle separated from the SMS. b) G-SMS gel after the fibrillation process using grinding at a concentration of 6.5 wt.%, (b′) optical microscopy image showing the degree of fibrillation, (b″) SEM micrograph showing the microstructure of G-SMS after grinding. c) E-SMS material after extrusion process at a concentration of 38 wt%, (c′) optical microscopy image showing the degree of fibrillation, and (c″) SEM micrograph showing the microstructure of E-SMS.

After mushroom harvest the lignin content was reduced between 74–77% and that of xylan by 62–72%. The chemical compositions of SMS we used as starting material can be found in Xiong et al.[32] SMS was not further chemically pretreated nor extracted prior to fibrillation. For G-SMS pulp the radical scavenging activity was determined to be 100% at the highest material concentration (Figure 3b), signifying clear antioxidant activity after 20 h of incubation, yet the activity was pronounced already after 30 min (Figure S1, Supporting Information). The pulp produced from SMS comprised mainly degraded wood, whose major component is cellulose, but also residual mycelium, as indicated by the low nitrogen content (1 wt.%), shown in Figure 3c. The nitrogen content of raw birch without any mycelium present was only 0.2 wt% (Table S2, Supporting Information). In Figure 3d, the ssNMR peaks at 21 and 171 ppm assigned to methyl carbons and C=O carbons associated with chitin are present, although less pronounced compared to their peaks in MR after alkali extraction. Peaks in the range of 30–33 ppm in the ssNMR spectrum of all fungal pulps and G-SMS pulp indicate the presence of proteins and lipids from the fungal cell wall,[47] which were not present in raw birch wood (Figure S2, Supporting Information). The ssNMR spectrum of G-SMS pulp showed the C1–C6 peaks of cellulose. In contrast to MR pulp, C4 and C6 in the range of 84–89 ppm and 62–65 ppm, respectively, were assigned to the interior (i) and surfaces (s) of crystalline cellulose domains.[48] The methoxy methyl carbons and aromatic and C=C carbon originating from lignin were observed at 56 ppm and 150–154 ppm.[49]

2.2. Flexible Sheets from Mushroom Residue

The properties required of cosmetical face masks are flexibility combined with sufficient strength, foldability (to enable packaging), wettability, high water absorption and retention, and sensory properties including softness and adhesion, and ideally moisturizing and skin-rejuvenating properties.[50,51] MR sheets containing antioxidants were the reason to explore them to produce cosmetic face masks. **Figure** 4a shows the resulting flexible

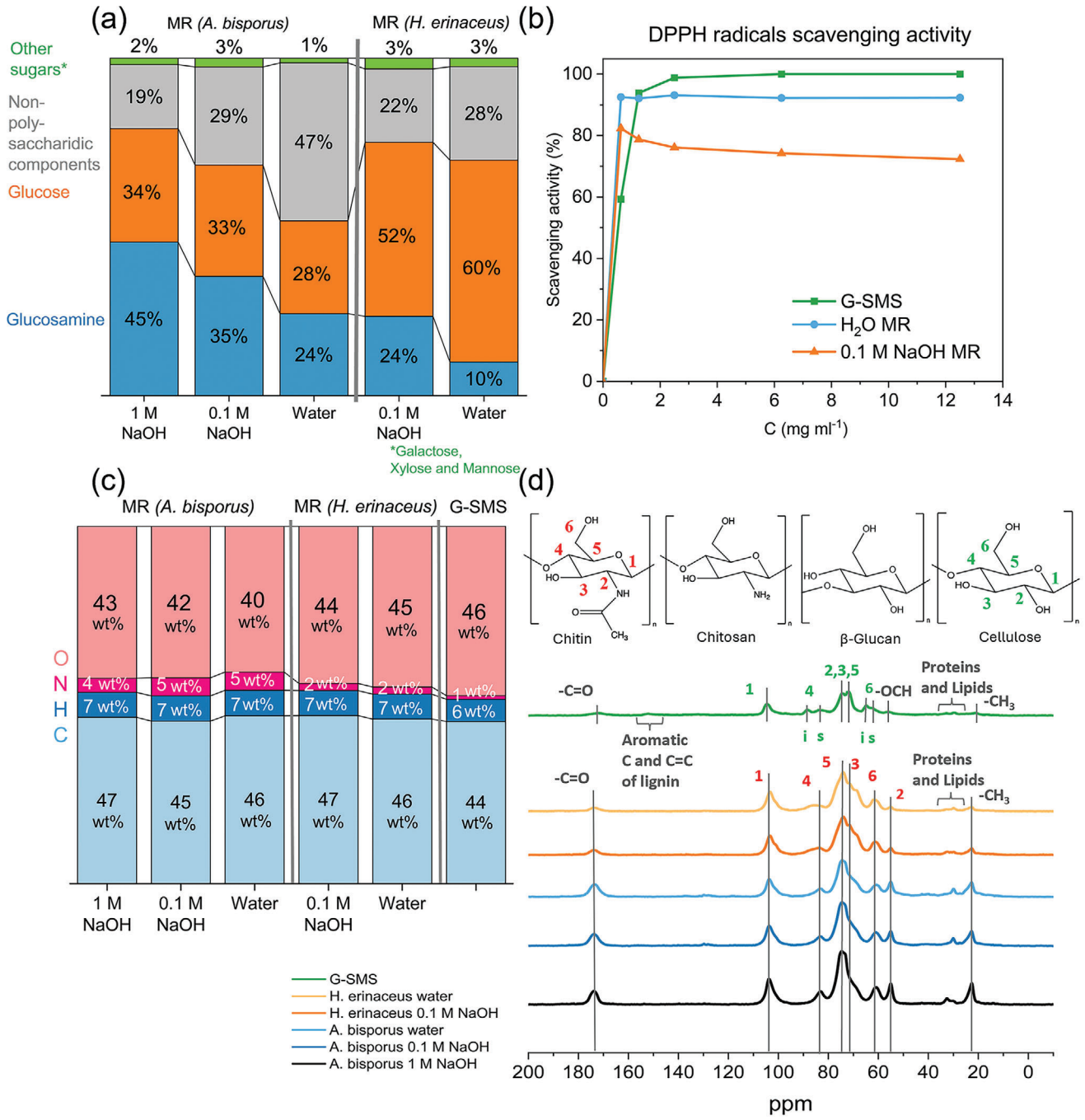

Figure 3. a) Carbohydrate analysis of MR pulp including glucose, glucosamine, other sugars including galactose, xylose, and mannose, and other components such as proteins. b) Antioxidant activity, 2,2-diphenyl-1-picrylhydrazyl (DPPH) free radical scavenging of MR pulp, after water and NaOH extraction and SMS after fibrillation as a function of the concentration of material tested varying between 0.0625–12.5 mg mL^{-1} after 20 h of incubation. Samples were measured in triplicates and the average is presented. c) Elemental analysis (O, N, H, and C) and d) ssNMR spectra of MR extracted from *A. bisporus* and *H. erinaceus* using 1 M NaOH, 0.1 M NaOH and water, and of G-SMS. Samples were measured in 3–5 replicates and the average is presented.

and foldable MR sheets produced by glycerol-containing fungal pulp. MR sheets produced from *A. bisporus* pulp were light brown with a smooth surface. While surfaces of sheets produced from pulp obtained by 0.1 M NaOH extraction were homogeneous, those produced from pulp obtained by H_2O extraction were more inhomogeneous. As said previously (Figure 3a), fewer extractives were removed from the fungal biomass during extraction with water than in 0.1 M NaOH. This could result in lower connectivity between the chitin-glucan microfibrils, leading to the formation of inhomogeneous sheets. Sheets prepared from *H. erinaceus*

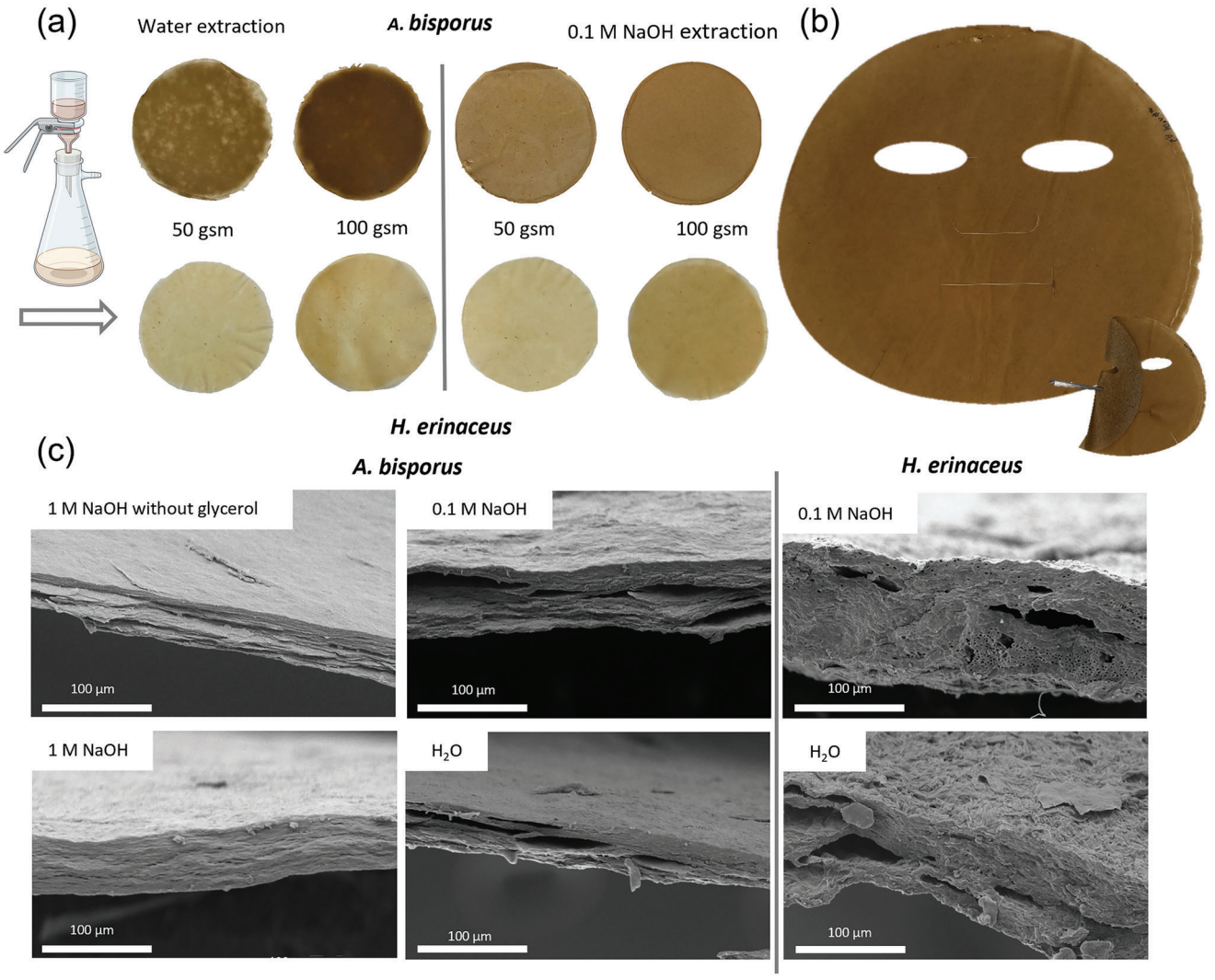

Figure 4. a) Flexible sheets after vacuum filtration, prepared from *A. bisporus* (upper row) and *H. erinaceus* (lower row) MR pulp extracted using hot distilled water (left) and 0.1 M NaOH (right) with target grammages of 50 and 100 g m^{-2} (image made with BioRender). b) Prototype of a fungal-based cosmetic face mask prepared from *A. bisporus*. c) SEM images of the cross-section of MR sheets (50 g m^{-2}) prepared from *A. bisporus* pulp obtained by extraction using 1 M NaOH (with and without the addition of glycerol), 0.1 M NaOH and hot distilled water and MR sheets prepared from *H. erinaceus* using 0.1 M NaOH and hot distilled water.

pulp were bright beige to sand color. The surfaces were slightly rougher than the sheets made from *A. bisporus*. To produce the cosmetic face masks, MR sheets can be prepared on a larger scale and cut to the facial features using a laser cutter as shown in Figure 4b. MR sheets prepared from *A. bisporus* pulp possessed a more layered and homogeneous structure than sheets made from *H. erinaceus* as shown in the cross-sections in Figure 4c. Plasticization of the fungal sheets using glycerol resulted in a reduced porosity, which dropped from 26 to 11% (Table S3, Supporting Information) and led to swelling of the sheet (thickness increased from 50 to 100 µm), which can be explained by the inclusion of glycerol between the fungal fibrils filling pores in MR sheets and increasing fibril-fibril distance.[52,53] The additional weight to the target grammage reflects the amount of glycerol included within the fibril network. For both mushroom types, sheets prepared from fungal pulp using NaOH extraction (0.1 or 1 M) had higher actual grammages and thus retained more glycerol within the network than sheets produced from pulp prepared by just water extraction. The glycerol content in the MR sheets prepared from *A. bisporus* with a target grammage of 50 g m^{-2} was determined to be 78 (± 3), 107 (± 40), and 27 (± 20) wt% for sheets produced from fungal pulp obtained by 1 M and 0.1 M NaOH and water extraction, respectively.

Sheets prepared from *H. erinaceus* had a spongy structure and heterogeneous surface with prominent structures of the fungal hyphae. MR sheets prepared from *H. erinaceus* pulp obtained using water extraction had the highest porosities with 37 and 27%. The porosity of sheets from *H. erinaceus* pulp was lower when extracted with 0.1 M NaOH, which decreased to 9 and 2% upon the addition of glycerol. The porosity is also affected by the target grammage; in all cases, sheets with a target grammage of 100 g m^{-2} had lower porosities than those with a target grammage of

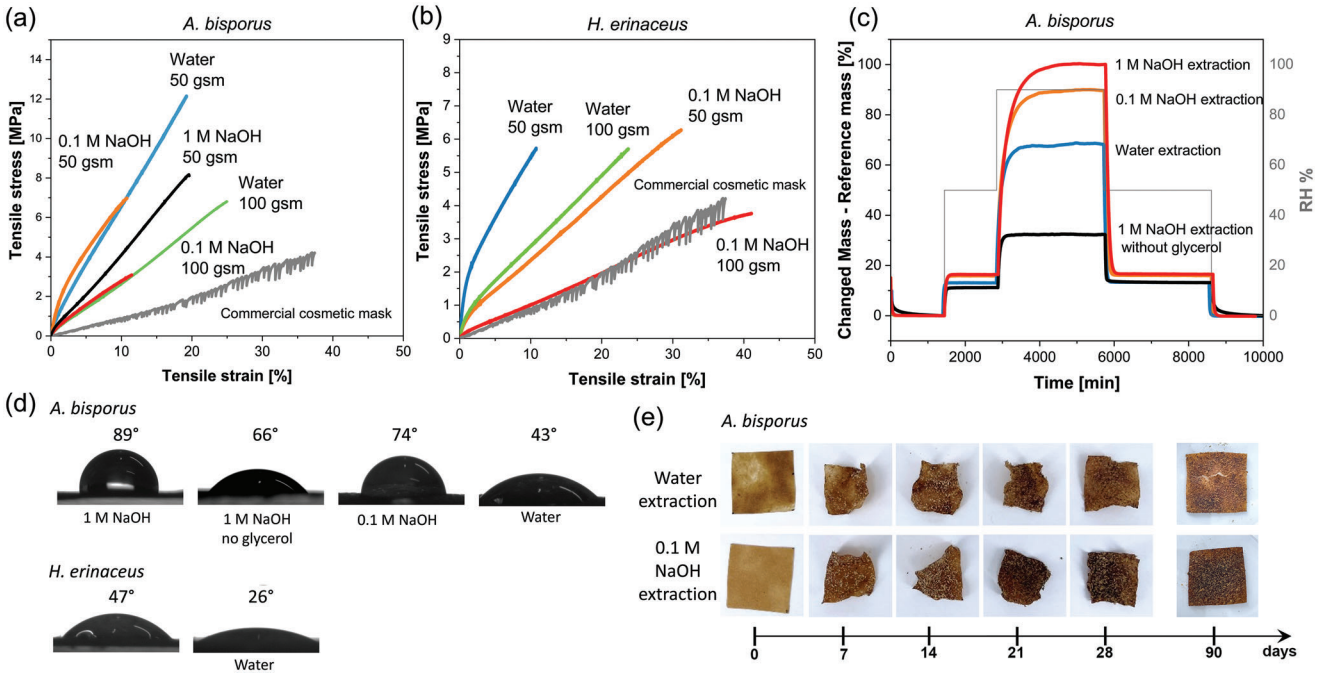

Figure 5. a) Representative stress-strain curves (n = 5–8) of flexible MR sheets with target grammages of 50 and 100 g m^{-2} produced from pulp obtained by water and 0.1 M NaOH extraction from *A. bisporus* and b) *H. erinaceus*, including a representative stress-strain curve of a commercial cosmetic mask. c) Dynamic vapor sorption of flexible MR sheets prepared from *H. erinaceus* biomass after extraction with water, 0.1 and 1 M NaOH (with and without glycerol) at 0, 50, 90, 50, and 0 RH%. d) Average initial water contact angle on flexible MR sheets prepared from *A. bisporus* and *H. erinaceus* (n = 30), e) Disintegration of MR sheets (50 g m^{-2}) prepared from *A. bisporus* pulp after water and 0.1 M NaOH extraction after 0, 7, 14, 21, 28, and 90 d in simulated compost.

50 g m^{-2}, which might be due to the higher amount of glycerol retained in thicker films during vacuum filtration. A commercial cosmetic mask had much higher porosity than all flexible MR sheets, resulting from the loose non-woven structure comprising plant fibers.

Representative stress-strain curves of the produced flexible MR sheets prepared from *A. bisporus*, *H. erinaceus*, and a commercial cosmetic mask are shown in **Figure** 5a,b, and sheet properties are summarized in Table S3 (Supporting Information). The sheet grammage determines the tensile modulus; for the same extraction method, sheets with a target grammage of 50 g m^{-2} always possessed higher tensile moduli than sheets with a target grammage of 100 g m^{-2}, aligning with the assumption that more glycerol is retained in higher grammage sheets, since glycerol increases fibril mobility, leading to lower tensile moduli.[52,53] When comparing flexible 50 g m^{-2} MR sheets, the tensile strengths were not significantly different from each other, except for MR sheets produced from *A. bisporus* using water extraction having the highest tensile strength of all flexible MR sheets. All flexible 50 g m^{-2} MR sheets significantly exceeded the tensile strength of commercial cosmetic masks. For flexible sheets with 100 g m^{-2}, sheets prepared using water extraction had higher tensile strength than sheets prepared from 0.1 M NaOH extraction. The commercial cosmetic mask had the lowest tensile strength and modulus but a high tensile strain of 41% and showed a stick-slip stress-strain behavior. Sheets with 100 g m^{-2} prepared from *H. erinaceus* using 0.1 M NaOH extraction have similar tensile strength and strain with up to 45% compared to the commercial cosmetic masks. The MR sheets prepared from *A. bisporus* pulp obtained by 1 M NaOH extraction without glycerol had a significantly higher average tensile strength of 47 MPa and tensile modulus of 6.5 GPa than sheets plasticized with glycerol and were brittle with tensile strains to failure of only 0.8% (Table S3, Supporting Information). As shown in Figure 5a, adding glycerol as a plasticizer resulted in a significant increase in tensile strain at the expense of tensile modulus and strength.

The amount of moisture absorbed by flexible *A. bisporus* sheets as a function of relative humidity and time is shown in Figure 5c. MR sheets produced from fungal pulp obtained by 1 M and 0.1 M NaOH extraction containing ≈70 wt.% glycerol absorbed most water albeit sorption equilibrium was only established after ≈2000 min. These sheets absorbed 100 and 90 wt% moisture, respectively, at 90 RH%. A lower glycerol content in the sheet prepared using pulp obtained from water extraction also results in a lower moisture uptake. MR sheets produced from fungal pulp obtained by 1 M NaOH extraction and without glycerol absorbed the least amount of water with 32 wt.% at 90 RH%, underlining the influence of the glycerol content in the sheets on water sorption. The water vapor permeability followed a similar trend; MR sheets prepared from *A. bisporus* pulps obtained by 0.1 M and 1 M NaOH extraction had higher water vapor permeabilities of 161 and 164 g h^{-1} m^{-2} as compared to sheets prepared from pulp obtained by water extraction with 146 g h^{-1} m^{-2} at 90 RH%. Pure MR sheets prepared using 1 M NaOH extraction without glycerol possessed a significantly lower vapor permeability of 67 g h^{-1} m^{-2} but exceeded vapor permeabilities reported for NFC films with

25–27 g h^{-1} m^{-2} at 90 RH%[54,55] and chitosan films with 41 g h^{-1} m^{-2} at 84 RH%.[56] Plasticization of MR sheets with glycerol resulted in better water transport through the MR sheets increasing the water vapor permeability. With increasing relative humidity, the water permeability of all fungal materials increases, less dramatically for E-SMS (Table S4, Supporting Information). Water droplets resting on MR sheets from which contact angles were determined are shown in Figure 5d. Pure *A. bisporus* MR sheets prepared using pulp obtained by extraction using 1 M NaOH had an initial contact angle of 66°, which dropped to 61° after 60 s (Table S5, Supporting Information) and were close to contact angles of 65° after 60 s reported by Nawawi et al.[9] for nanopapers made from chitin-glucan complex extracted from *A. bisporus*. The water contact angle increased to 89° when glycerol was added but decreased rapidly to 69° after 60 s, indicating fast water sorption by glycerol. The increased initial contact angles seem counterintuitive given that glycerol is completely miscible with water; water spreads on a glycerol surface and quickly dissolves (Video S1, Supporting Information). However, with increasing drying time, the surface of the plasticized sheets had a rougher topology, which could be the reason for the higher initial water contact angle of chitin-glucan sheets containing glycerol (78 wt%). Additionally, the lower porosity of MR sheets containing glycerol (Φ = 11%) than without glycerol (Φ = 32%) retard fast water imbibition. For the two fungi, pulp prepared from water extraction resulted in more hydrophilic sheets with water contact angles of 43° for *A. bisporus* and 26° for *H. erinaceus*. The hydrophilicity of the surfaces of the fungal sheets decreased when harsher extraction methods were used to prepare the pulp as more water- and alkali-soluble hydrophilic compounds were removed from the fungal biomass; for *A. bisporus* sheets the water contact angle increased from 43° to 74° and for *H. erinaceus* from 26° to 47°. The increase in water contact angles is attributed to the up-concentration of water- and alkali-insoluble protein hydrophobin[57,58] the harsher extraction method, leading to more hydrophobic surfaces. Compared to pure crustacean-derived chitin sheets, with reported water contact angles between 24° and 37°,[9,59] hydrophobin-coated glass surfaces were reported to have water contact angles between 62° and 77°.[60] MR sheets prepared from *A. bisporus* had higher water contact angles than MR sheets from *H. erinaceus*, which could also be attributable to the higher β-glucan content in *H. erincaeus* (Figure 3a). Biodegradability of single-use materials is important if they were to be (home) composted; both MR sheets prepared from *A. bisporus* pulp obtained by 0.1 M NaOH and water extraction did slowly disintegrate after 90 d as shown in Figure 5e.

2.3. Rigid Sheets from Spent Mushroom Substrate

SMS pulps produced by ultrafine grinding (G) or extrusion (E) were formed into sheets with a target grammage of 150 g m^{-2} using vacuum filtration followed by compression molding. The produced rigid sheets were visually distinguishable as shown in **Figure** 6a,b. The E-SMS sheets had two visually different sides; the side in contact with the filter paper appeared darker. Stereomicroscopy images provided in Figure S3 (Supporting Information) also confirmed the differences between two the sides of the E-SMS sheets. The G-SMS sheets had a thickness of 100 ± 10 µm and a density of 1.34 g cm^{-3} while the E-SMS sheets at a thickness of 150 ± 20 µm, and a density of 1.09 g cm^{-3} confirming that E-SMS sheets had a higher porosity, 28% compared to G-SMS sheets with only 9%. SEM micrographs of the cross-section of the sheets are presented in Figure 6a′,b′, showing that the G-SMS sheets were indeed better packed compared to E-SMS sheets, in which the fibers are difficult to distinguish since they appear to be partly embedded in fungal microfibrils. These images agree with the density and porosity measurements, as well as fiber size analysis, previously discussed (Figure 2). The reason behind the better packing of G-SMS, in comparison to E-SMS sheets, can be explained by their smaller fiber size and the absence of large intact structures. G-SMS sheets absorbed ≈7 wt% of water at 50 RH% and ≈17 wt% at 90 RH% (Figure 6c). E-SMS sheets adsorbed comparable amounts of moisture; ≈8 wt% at 50 RH% and ≈18 wt% at 90 RH%. The wettability of the sheets was assessed by measuring the water contact angles of droplets resting on the films (Figure 6d) on the side in contact with the filter paper upon filtration. The G-SMS sheets were slightly more hydrophobic with contact angles of 92° compared to that of E-SMS with 85°. The G-SMS retained contact angles of 89° after 60 s while those of E-SMS sheets dropped to 61° (Table S6, Supporting Information). Characteristic stress-strain curves of the SMS sheets are shown in Figure 6e and the corresponding data is in Table S7 (Supporting Information). Ultrafine grinding resulted in sheets (G-SMS) having a tensile strength of 42 MPa and elastic modulus of 5 GPa, which were much higher than those of the E-SMS sheets (strength of 9 MPa, and E-modulus of 2 GPa). The reason is that the G-SMS sheet comprised smaller and longer fibers which resulted in many more fiber-fiber contacts in the network as compared with the fiber network of E-SMS. However, the properties of the E-SMS sheet are still similar to paper made of commercial bleached Kraft birch pulp having a strength of 16 MPa and an E-modulus of 1.3 GPa.[61] Both SMS sheets were rigid and brittle, having a strain to failure of ≈1%.

Today's single-use plastic packaging materials are often discarded and leak into nature[62] requiring alternatives to replace persistent polymer materials. We evaluated the potential of G-SMS sheets for packaging applications by comparing their properties with polylactic acid (PLA) sheets. Photographs of the G-SMS and PLA sheets are shown in **Figure** 7a; G-SMS sheets have a plastic-like appearance having a smooth surface but are brown in color. The reason is the fine fibril network together with the remaining fungal hyphae in the SMS pulp, which is expected to act as a binder between the wood fibrils.[37] PLA is a common renewable packaging material but still adds to the microplastic pollution as it is only biodegradable in industrial composting conditions but not in seawater.[63] The SMS sheets have several benefits compared to polymeric packaging materials; they are biobased, low cost, and possess low oxygen permeability when tested in a dry state with inlet pressures varying from 1 to 5 bar. The antioxidant activity of these materials could be beneficial for using these SMS sheets as biobased and bioactive packaging. Figure 7b shows that the G-SMS sheet displayed lower water wettability compared to PLA, which had contact angles of 69° (Table S5, Supporting Information). G-SMS sheets possessed similar tensile strength, but higher modulus (5 GPa) when compared with PLA (see Figure 7c). PLA films started to disintegrate within 21

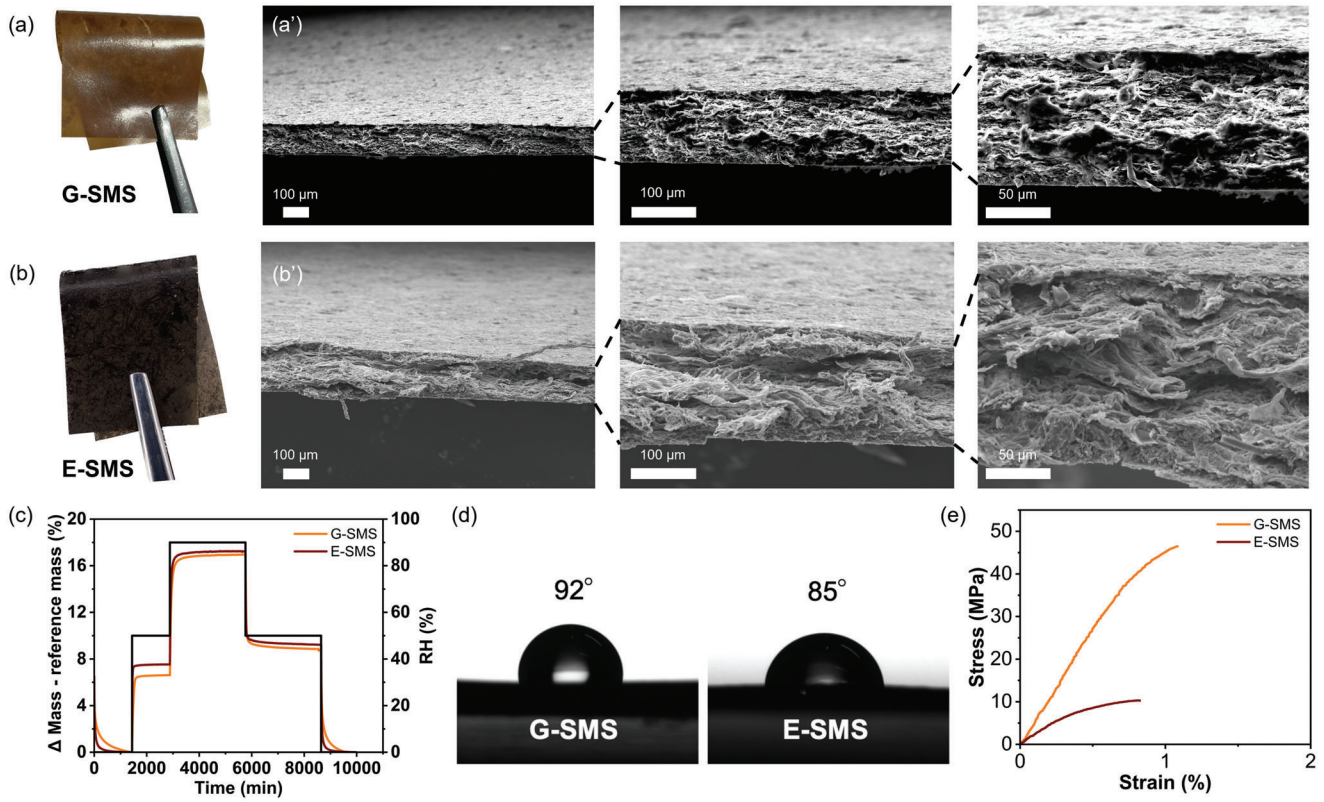

Figure 6. Photographs of rigid sheets produced by vacuum filtration and compression molding of a) G-SMS and b) E-SMS pulp. SEM micrographs of the cross-section of (a′) G-SMS and (b′) E-SMS sheets. c) Dynamic vapor sorption curves of rigid G-SMS and E-SMS sheets. d) Water droplets resting on rigid sheets prepared from G-SMS and E-SMS measured after 1 s (n = 30). e) Representative stress-strain curves of G-SMS and E-SMS sheets (n = 5).

d in simulated compost (see Figure 7d) and near complete disintegration was observed at day 90 while the SMS sheet did not disintegrate in these conditions since SMS material is mainly composed of ground wood, which only slowly degrades in nature. The G-SMS sheets disintegrated in water after 2 d under gentle magnetic stirring (see Figure S4 and Video S2, Supporting Information).

2.4. Spent Mushroom Substrate Foams

G-SMS pulp was processed into foams by pouring the pulp suspension into a mold, freezing at −25 °C, and then freeze-dried as shown schematically in **Figure** 8a. The high porosity foams (Φ = 95%) consist of a 3D network of interconnected fibers, see Figure 8b. The foam density was 0.09 ± 0.01 kg m^{-3} and its specific surface area (SSA) was only 4.4 m^2 g^{-1}. The compression stress-strain curves of the produced foams are shown in Figure 8c. SMS foams had a compression strength $\sigma_{50\%}$ of 53 ± 3 kPa, and modulus ($E_{<5\%}$) of 111 ± 22 kPa, similar to those previously reported for crosslinked cellulose nanofiber/hemicellulose aerogels.[64] The relatively high density and mycelium binder may be the reasons for these properties. Naturally degrading sorbents are of interest for example, for the removal of oil spills because these will not add to microplastic pollution in nature.[65] Different natural materials such as rice husk, peat, straw, corncobs, sawdust, etc. have been studied, however, these materials are very hydrophilic and generally need to be modified to enable oil absorption. Cellulose-based aerogels/foams exhibit high porosity, high specific surface area, low density, and very high absorption capacity however limited to water. To facilitate oil uptake, these need to be chemically modified to render the material hydrophobic.[66]

We evaluated the G-SMS foams as a completely natural oil absorbent that would not lead to microplastic pollution if left unintentionally in nature. Water and oil absorption capacities of G-SMS foams are shown in Figure 8d. The foam absorbed water up to 21 times its initial weight after 5 min immersion and engine oil up to 28 times its weight. The foams were still stable after 5 min of immersion in both fluids, suggesting good network formation; after removing the foam from water it slightly deformed while when removed from oil the foam did not deform, suggesting better oil stability. Separation of engine oil from water was also performed, as shown in Figure 8e; the oil was colored red and spread on the water surface. The foam was submerged into the medium, and after a few seconds, the foam successfully absorbed the spilled oil from the water without collapsing. Oil spills due to crude oil exploration and transportation cause significant environmental issues. Both hydrophobic and oleophilic porous materials have been explored for oil spill remediation.[67] SMS foams, having both hydrophilic and oleophilic characteristics without any chemical modification, could potentially be used for both water and oil sorption.

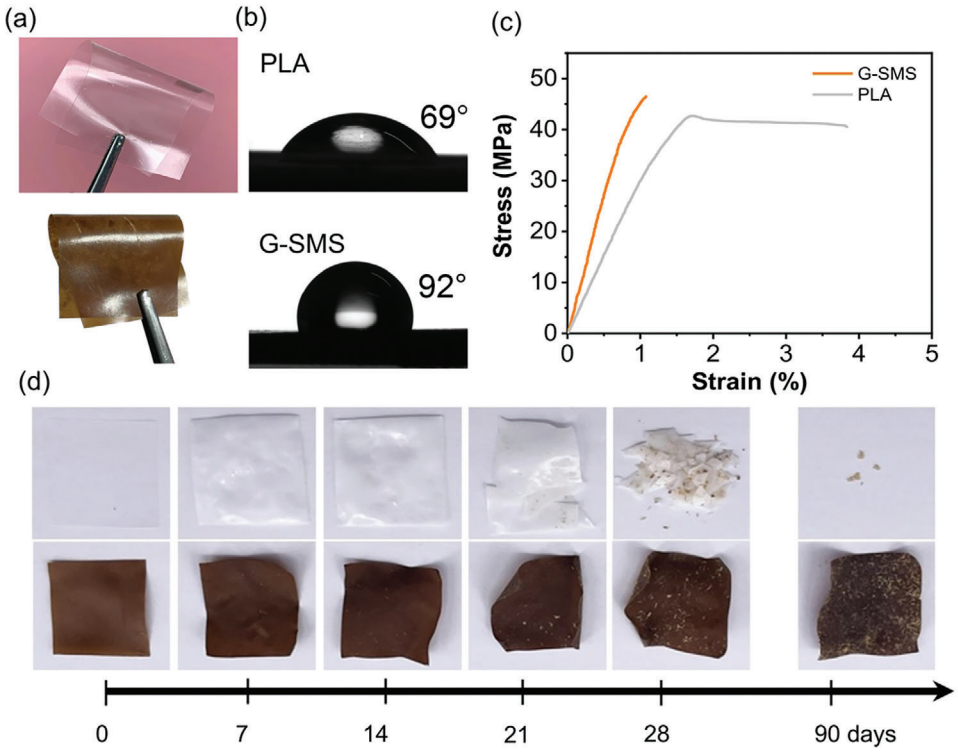

Figure 7. Comparison of PLA and SMS sheets a) photographs of the films. b) Water droplets resting on those films (n = 30) c) Representative stress-strain curves (n = 5) d) Appearance of PLA films and G-SMS sheets during disintegration under composting conditions.

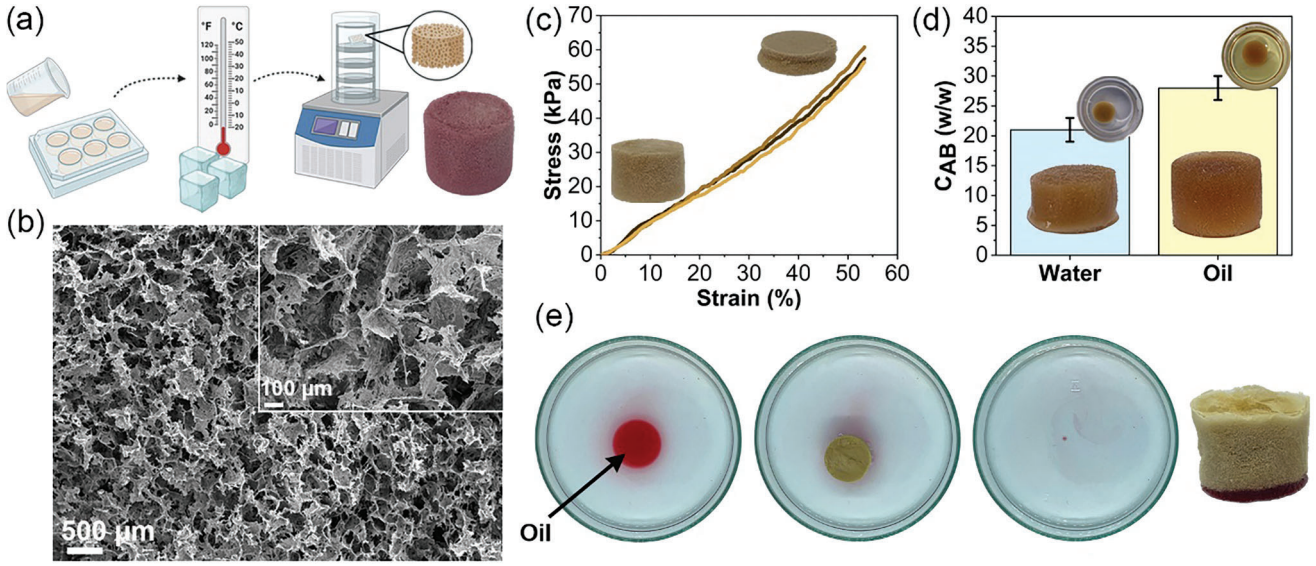

Figure 8. a) Schematic illustration of G-SMS foam production (illustration made using Bio Render). b) Low and high magnification SEM of the foam cross-section showing its open pore structure and a 3D fiber network. c) Compression stress-strain curves, showing the foam before and after the test (n = 5). d) Water and oil absorption capability of the foams (n = 5) together with photographs of foams after being 5 min immersed into each fluid. e) Sequence of photos where the foam was used to remove red-colored oil from water, and photographs of the foam after removal, where the absorbed (red-colored) oil is seen at the bottom of the foam.

3. Conclusion

In conclusion, resource-efficient fungal biomass, namely mushroom residues (MR) and spent mushroom substrate (SMS), can be turned into sustainable and functional materials. We demonstrated that it is feasible to produce flexible sheets from fungal pulp made from fruiting bodies plasticized using glycerol for use as cosmetic face masks. The developed masks have antioxidative properties, and sufficient mechanical properties for their intended use. The extraction methods used to produce the fungal pulp do influence the properties of the pulp fibers, such as their morphology, chemical, mechanical, and surface properties. The preparation of MR sheets from the pulp of *A. bisporus* produced by water extraction resulted in masks that were more suitable for cosmetic applications, due to their higher strength, strain, and better wettability. Additionally, sheets prepared by pulp obtained by simple hot water extraction exhibit higher antioxidative properties. The potential of using other mushroom types, such as *H. erinaceus*, was demonstrated. The SMS after shiitake mushroom cultivation was fibrillated using ultra-fine grinding (G-SMS) and co-rotating twin-screw extrusion (E-SMS). The different techniques had different processing efficiencies, sheet appearance, and properties. Both processes resulted in greatly reduced SMS fiber size without needing to use additional chemicals. Ultrafine grinding resulted in the finest fibrils. The extrusion process was more efficient as a high solid content could be processed in a short time compared to grinding. The strength and stiffness of the G-SMS sheets were comparable to PLA, while the E-SMS sheets possessed much lower mechanical properties and a very dark color but were comparable to commercial bleached birch pulp paper. The contact angles for the sheets were 85° for E-SMS sheets and 92° for G-SMS sheets, showing that G-SMS sheets were more hydrophobic. Also, G-SMS sheets possessed antioxidant activity and low permeability when tested in dry conditions and at room temperature. In addition, the G-SMS sheets were smooth and had a polymer-like appearance. Composting trials demonstrated that G-SMS and MR sheets remained intact even after 90 days, showing good long-term properties. Foams with amphiphilic behavior could also be prepared from G-SMS pulp. These foams sorbed both water and oil and effectively separated oil from water.

4. Experimental Section

Mushroom Residues (MR): *A. bisporus* (white button mushroom) was purchased in local stores in Vienna (origin: B. Fungi Kft, Ocsa, Hungary). *H. erinaceus* (lion's mane mushroom) was cultivated at the Institute of Material Chemistry of the University of Vienna and frozen (−18 °C) after harvest.

Commercial Cosmetic Mask: Compressed Akliocss one-way nonwoven facial masks made from fleece cotton from Akissco-de (Guangdong, China) were purchased over amazon.com, Inc. Masks were soaked in water to decompress and dried before measurement.

Spent Mushroom Substrate (SMS): The used SMS material comprised birch (*Betula pubescens*) particles for bench-scale cultivation of shiitake (*Lentinula edodes*) produced at the Mushroom laboratory at the Swedish University of Agricultural Sciences, (SLU), Umeå, Sweden. The SMS was collected and frozen (−18 °C) after harvest.

Reference Packaging Material: Polylactic acid (PLA), from NatureWorks Ingeo 4043D (Minnetonka, MN, USA), was used as a reference packaging material.

Chemicals: Distilled water was used for all experiments. Sodium hydroxide (NaOH ≥ 97.0%) and glycerol 1.26 were bought from Wilhelm Neuber's Enkel Dr. Brunner & Kolb GmbH, (Vienna, Austria), and used as received. Engine oil Castrol Edge OW-30 with a density of 0.842 g ml^{-1} and viscosity of 72 mm^2 s^{-1} (40 °C) was used to investigate oil absorption. The red dye Oil Red O (Sigma–Aldrich Sweden AB, Solna, Sweden) was used to color the engine oil for oil removal from water. Sugar recovery standard were prepared from D-(+)-galactose, D-(+)-xylose and D-(+)-mannose from Merck, D-(+)-glucose and L-(+)-rhamnose from BDH Prolabo, L-(+)-arabinose from Calbiochem and D-(+)-glucosamine hydrochloride (Sigma-Aldrich Finland Oy, Helsinki, Finland).

Fibrillation of MR and Extraction: Two different types of fungi were used: *A. bisporus* and *H. erinaceus*. 500 g of fruiting bodies were washed twice and blended for 3 min in 500 ml distilled water using a kitchen blender (Tristar, BL-4473 VitaPower 2000). Two chitin-glucan extraction methods were tested. The produced fungal biomass suspension was either extracted in hot 2 L 0.1 M NaOH at 65 °C for 0.5 h followed by cooling to 25 °C and washing with distilled water using vacuum filtration through a cotton fabric in a Büchner funnel until neutral pH. To retain as many valuable fungal components as possible for cosmetic applications, the fungal biomass was only extracted in 2 L hot distilled H_2O (65 °C) for 0.5 h. For comparison, the standard extraction method reported by Nawawi et al.[18] was used for *A. bisporus*; fruiting bodies were heated in dist. Water at 85 °C for 0.5 h before heating in 1 M NaOH at 65 °C for 3 h. To determine the dry mass content (*DM*) samples with ≈0.5 g of biomass were weighed in a wet state (m_w) and again after drying in an oven at 70 °C overnight (m_d) Equation 1. The average of the three samples was taken for the calculation of the dry mass content in %:

$$DM = \frac{m_d}{m_w} \times 100 \quad (1)$$

The produced fungal pulp was stored at 4 °C prior to use.

Preparation of Flexible MR Sheets: Flexible MR sheets targeting a grammage of 50 and 100 g m^{-2} were prepared for application as fungi-based cosmetic masks. The respective amount of biopolymer was blended (Tristar, BL-4473 VitaPower 2000) for 1 min with 100 ml distilled water and 30 ml glycerol and vacuum filtrated through a Duran sintered disc filter funnel with porosity 2 (Th. Geyer GmbH & Co. KG, Renningen, Germany) and a filter paper (VWR 413, qualitative filter paper, particle retention 5–13 µm, Lutterworth, UK) using a water vacuum pump. The sheets were removed from the filter paper and placed in a sandwich structure between thin-meshed metal nets, and blotting paper (3 MM Chr VWR, Lutterworth, UK) before drying between two metal plates with a weight of 5 kg on top at 50 °C on a heating plate. Sheets with 50 g m^{-2} were dried for 24 h and sheets with 100 g m^{-2} for 48 h with changing blotting paper in between.

Fibrillation of the SMS: The frozen SMS was defrosted at room temperature (23 °C) for ≈16 h before being manually disintegrated and then soaked in 50 °C warm water for 1–5 d. The water was changed to fresh water and excess water in the material was squeezed manually. Two different fibrillation processes were tested, as follows: *G-SMS*: The SMS with 6.5 wt% solid content was dispersed using mixer (Ystral GmbH, Ballrechten-Dottingen, Germany) for 10 min prior to fibrillation using an ultra-fine grinder (G) (MKZA6-3, Masuko Sangyo Co., Ltd., Kawaguchi, Japan) equipped with coarse silica carbide (SiC) grinding stones. The fibrillation was conducted in contact mode, with the gap of the two discs set to contact and then gradually adjusted to -90 µm at 1500 rpm. *E-SMS*: The SMS was concentrated to 28 wt% and manually fed into a co-rotating twin-screw extruder (E) (Coperion W&P ZSK-18 MEGALab, Stuttgart, Germany). The temperature was set to 90 °C at the start and 110 °C at the die and the screw speed to 120 rpm which resulted in a residence time of 3 min.

Preparation of Rigid SMS Sheets: Rigid SMS sheets with a target grammage of 150 g m^{-2} were prepared from the pulps after the two fibrillation processes. The pulps were diluted with distilled water and stirred for 30 min. The suspensions from different fibrillation techniques were vacuum filtrated through a membrane filter (Durapore PVDF 0.1 µm pore

size, from Millipore, Darmstadt, Germany) using a vacuum pump (VCP 80, VWR International AB, Stockholm, Sweden). All sheets were placed between aluminum plates (300 mm x 300 mm), paper, and thin-meshed metal nets (pore size 50 µm). Sheets were dried in a vacuum oven (NSV 9000, LABEX, Helsingborg, Sweden) for 30 min under a weight of 5 kg at 80 °C. The sheets were placed between Mylar films (Lohmann Technologies, Milton Keynes, UK) and aluminum plates, and kept in a compression molding machine (LabEcon 300, Fontijne Press, Vlaardingen, The Netherlands) at 100 °C, pressed for 10 min at 2.5 MPa and cooled down to 20 °C at the same pressure. The average thickness of G-SMS and E-SMS were ≈100 µm and 150 µm, respectively.

Preparation of Reference Packaging Material: PLA film was prepared using the same compression molding machine (LabEcon 300, Fontijne Press, Vlaardingen, The Netherlands). PLA pellets (4 g) were placed between Mylar films and aluminum plates, pre-heated at 190 °C for 240 s, and then compression-molded with a pressure of 2.5 MPa for 60 s at the same temperature, followed by cooling down to 20 °C at the same pressure for 5 min. The film's average thickness was 120 µm.

Preparation of SMS Foams: G-SMS pulp was diluted in water to 3 wt% and magnetically stirred for 1 h. The suspensions were poured into a mold and placed into a freezer (−25 °C) for 15 h, followed by freeze-drying using a Martin Christ Alpha 1–4 LSC plus freeze dryer (Svenska LABEX AB, Helsingborg, Sweden), where the frozen samples were subjected to a pressure of 1 mbar (−55 °C) for 40 h, followed by a final drying where the pressure was set to 0.1 mbar for 1 h.

Fiber Size Measurement: The fiber dimensions of G-SMS and E-SMS were investigated using a F5S Valmet Fiber Image Analyzer (Valmet Automation Oy, Kajaani, Finland). To analyze the dimensions, fiber suspensions were diluted to 10 mg L^{-1} and ≈3000 images were captured where 30 000 to 60 000 fibers were analyzed. The fibers were divided in six different fractions, starting with fraction 1 (0–0.2 mm), fraction 2 (0.2–0.6 mm), fraction 3 (0.6–1.2 mm), fraction 4 (1.2–2.0 mm), fraction 5 (2.0–3.2 mm) and fraction 6 (3.2–7.6 mm).

Optical Microscopy: Optical examination on MR, G-SMS, and E-SMS fibers was carried out using Nikon Eclipse LV100N POL (BergmanLabora AB, Danderyd, Sweden) and images were captured using the imaging software NIS-Elements D 4.30. All samples were investigated at a 4 and 10-times magnification. MR pulp was diluted to 0.4 wt% and the diameter of water-swollen fungal hyphae was determined from optical microscopy images using ImageJ (n = 100). G-SMS and E-SMS pulp were diluted to 0.25 wt% after fibrillation processes prior to the observation.

Scanning Electron Microscopy (SEM): MR and SMS pulp (before and after the fibrillation) were diluted to 0.1 wt% and dropped onto a carbon tape placed on the sample holder using a pipette, subsequently freezing in liquid nitrogen, and freeze-dried using the Martin Christ Alpha 1–4 LSC plus freeze dryer (LABEX AB, Helsingborg, Sweden) in two different steps. The samples were first dried under −55 °C and at a pressure of 1 mbar for 40 h and the pressure was further reduced to 0.1 mbar for 1 h. For high-resolution microscopy of E-SMS and G-SMS, (Magellan 400 XHR–SEM, FEI Company, Hillsboro, OR, USA) was used, at an acceleration voltage of 0.35 kV without applying any coating for visualization of the fibrillated natural structures. All other samples were sputtered with platinum to a layer of 15 nm using EM ACE200 (Leica, Wetzlar, Germany) and the samples were analyzed using JEOL JSM-6460LV (Jeol Nordic AB, Sollentuna, Sweden). The images were acquired in high vacuum at an acceleration voltage of 5 kV and 15 kV detecting the secondary electrons to obtain the morphology information. To analyze the cross-section of MR sheets, sheets were dried for 12 h under vacuum at 70 °C before cryo-fracturing them in liquid nitrogen. Samples were placed on a carbon tape and sputtered with gold using a fine coater JFC-1200 (JEOL GmbH, Freising, Germany) before imaging using NeoScope JCM-7000 (JEOL GmbH, Freising, Germany) with an accelerating voltage of 30 kV. The cryo-fractured cross-section of G-SMS and E-SMS sheets were sputter-coated with a 15 nm Pt layer and G-SMS foams were cut using a fresh microtome blade and sputter-coated with a 10 nm Pt layer using EM ACE200 (Leica, Wetzlar, Germany) and investigated using JEOL JSM-6460LV (Jeol Nordic AB, Sollentuna, Sweden).

Viscosity Measurement: The viscosity of SMS pulps was measured using a Vibro-Viscometer SV-10 (A&D Company, Oxford, UK) at concentrations of 6.5 wt% for G-SMS and E-SMS at 21 °C. All samples were measured as triplicate for a duration of 2 min each after the plateau was reached, and the average viscosity was reported with standard deviations.

Sugar Analysis: Sugar analysis was performed on MR using high-performance anion exchange chromatography (HPAEC). Freeze-dried pulps (300 mg) were stirred in 3 mL sulfuric acid (72%) at 30 °C for 1 h. The mixture was diluted with H_2O to 4% before autoclaving at 121 °C for 1 h. Sugar recovery standards were prepared under the same conditions. HPAEC was carried out using a Dionex ICS3000 chromatograph with a CarboPac PA20 column (ThermoFisher Scientific, Vantaa, Finland).

Antioxidant Activity in MR and SMS: The 2,2-diphenyl-1-picrylhydrazyl (DPPH) radical scavenging activity of the MR and SMS materials after extraction and fibrillation process respectively, were assayed according to Xu et al.[68] An adequate amount of freeze-dried material was weighed in a tube and 0.4 mL distilled water was added. The mixture was shaken vigorously. Then, 0.4 mL of 0.2 mM DPPH ethanol solution was added. The final concentration of freeze-dried material varied between 0.0625−12.5 mg mL^{-1}. The final concentration of DPPH was 0.1 mM. A series of blank samples was prepared containing 0.4 mL of distilled water and 0.4 mL of 0.2 mM DPPH ethanol solution. A series of blank samples were prepared containing the materials without DPPH adding 0.4 mL distilled water and 0.4 mL ethanol. The final mixtures were shaken at 1000 rpm and room temperature in the dark. At 30 min and 20 h, a homogeneous aliquot was withdrawn, and the sample mixture was centrifuged for 2 min at 5000 rpm to remove the hydrogel solids. The supernatant was pipetted into a 96-well plate and its absorbance at 517 nm was measured via a microplate reader, in triplicates. The DPPH radicals scavenging activity (RSA) was calculated as follows (Equation 2):

$$DPPH\ RSA = \left[1 - \frac{A_S - A_1}{A_0}\right] \times 100 \quad (2)$$

where A_S is the absorbance of the sample and DPPH, A_1 is the absorbance of the sample (hydrogel in water: ethanol 50:50 v/v), and A_0 is the absorbance of the control (DPPH 0.1 mM in water: ethanol 50: 50 v/v).

Elemental Analysis: MR pulp (dried at 80 °C overnight) and SMS foams were ground to a fine powder using a mortar prior to measurement. Elemental Analyses were performed by Mikroanalytisches Laboratorium, University of Vienna. An EA3000 (Eurovector Pavia, PV, Italy) was used for C/H/N/S-analysis. This instrument uses flash combustion to digest the material at 1.000 °C. The detection and quantification of nitrogen, carbon dioxide, water, and sulfur dioxide were done after chromatographic separation using a Thermal Conductivity Detector (TCD). A high-temperature pyrolysis oven HT-1500 (HEKAtech GmbH, Wegberg, Germany) was used to digest the material and release oxygen as carbon monoxide which was detected using the above instrument. The evaluation was based on calibration using only certified standard materials. Triplicate measurements each based on a sample equivalent of 1 to 2.5 mg were made to identify variation caused by heterogeneity.

Solid State Nuclear Magnetic Resonance (ssNMR): MR pulp was dried at 80 °C overnight and SMS foams were ground to a fine powder using a mortar prior to measurement. 13.2 mg of sample were inserted into a 12 µl Zirconium Dioxide Rotor with a KEL-F cap. ssNMR spectroscopy was performed using an AV NEO 500 WB, Bruker BioSpin, Bruker BioSpin GmbH & Co.KG, Ettlingen, Germany (with a widebore system at 298.2 K. A 2.5 mm MAS probe was utilized, operating at a resonance frequency of 125.78 MHz.

Mechanical Properties: Sheets from MR were cut (Zwick ZCP 020 Manual Cutting Press, Zwick, Ulm, Germany) into dog bone-shaped specimens with a parallel width of 5 mm and an overall length of 75 mm (Type 1BA, EN ISO 527-2). The thickness of dog bone-shaped specimens was determined with a micrometer gauge (Digital Outside Micrometre 0–25 mm, AnyiMeasuring, Guilin City, P.R. China). All the sample thicknesses were measured 3–4 times at random locations at the parallel section of the

specimen. For MR sheets, Young's modulus, tensile strength, and strain to failure were determined by tensile tests using an Instron universal test frame (Model 5969 Column Universal Testing System, Instron, Darmstadt, Germany) equipped with a 1 kN load cell, and a strain rate of 1 mm min^{-1} and a gauge length of 25 mm. The Young's modulus was determined by the slope of the linear elastic region and the tensile strength was calculated by dividing the maximum load by the cross-sectional area of the specimen. The corresponding engineering strain was defined as the strain to failure. 5–8 specimens were tested for each material and results were presented as average. Statistical analysis was performed using one-way analysis of variance (ANOVA) and Tukey's test at a 5% significance level. Open source Past4 software, version 4.12b (Natural History Museum, University of Oslo, Norway) was used. Tensile samples for G-SMS, E-SMS, and PLA were cut into rectangular samples of 50 mm x 5.9 mm using a punch. The samples were conditioned at 50% relative humidity at 22 °C for at least 48 h prior to testing. The sample thickness was measured 3–4 times at random locations at the parallel section of the specimen using a micrometer gauge (Digital Outside Micrometre 0–25 mm, AnyiMeasuring, Guilin City, P.R. China). The tensile properties were measured using a Shimadzu AGX-V universal testing machine (BergmanLabora, Danderyd, Sweden) equipped with a non-contact video extensometer (TRViewX, Shimadzu, BergmanLabora, Danderyd, Sweden) and 500 N load cell. A gauge length of 30 mm and strain rate of 3 mm min^{-1} were applied. The results were averages of at least 5 sets of measurements for each prepared sheet. Statistical analysis was performed using one-way analysis of variance (ANOVA) and Tukey's test at a 5% significance level. Open source Past4 software, version 4.12b (Natural History Museum, University of Oslo, Norway) was used. Cylindrical SMS foams with a height of 15 mm were tested under compression an Instron 4411 Series (Instron, Norwood, MA, USA) at a strain rate of 10% min^{-1} with a 500 N load cell. The modulus ($E_{<5\%}$) was calculated from the linear region of the stress-strain curve between 3–5% strain. At least 5 samples were tested, and the average was presented.

Glycerol Content: The glycerol content of flexible MR sheets prepared from pulp of *A. bisporus* obtained from water, 0.1 and 1 M NaOH extraction was determined using dynamic vapor sorption (DVS Resolution, Surface Measurement Systems, London, UK). The mass change at 0% RH for 27 h was measured to dry the samples. 3 samples per extraction method were measured and the average was presented. The actual dry weight over the target weight was attributed to the amount of glycerol in the MR sheet.

Water Vapor Uptake: The water vapor sorption was analyzed for MR, G-SMS, E-SMS, and PLA sheets using dynamic vapor sorption (DVS Resolution, Surface Measurement Systems, London, UK). This was done by cutting 10–20 mg of each sample into ≈2×2 mm^2 pieces and measuring their change in mass at 0, 50, and 90% RH and cycling back to 50% and 0% RH at 25 °C. Each sample was measured once.

Water Contact Angle Measurements: *MR, SMS, and PLA sheets*: The water contact angle was measured for MR, G-SMS, E-SMS, and PLA sheets using a drop shape analyzer (DSA30, Krüss GmbH, Hamburg, Germany) with a dose volume of 5 µl and dosing rate of 16 μls^{-1}. The contact angles after a delay of 0, 1, 5, 15, 30, and 60 s were measured on 30 replicates per material, and the average was presented. The water contact angle measurement of MR sheets from 1 M NaOH extraction (with and without glycerol) was repeated by three people with measurements of 30 drops per sheet to confirm the result.

Disintegration Test: The degree of disintegration of MR prepared using 0.1 NaOH and water, and G-SMS and PLA sheets were studied following standard ISO-20200. The prepared sheets were cut into 6 individual pieces (25 × 25 mm^2) for each material and dried in a vacuum oven (NSV 9000, LABEX AB, Helsingborg, Sweden) at 40 °C until the weight was constant. The individual weight of the pieces was measured and recorded. Each piece was placed inside a polyester bag (mesh size: 1.7 mm), as previously described by Arrieta et al.[69] and placed in a reactor (30 × 20 × 15 cm^3), where the samples were buried at 5–6 cm depth. The reactor was incubated inside an air circulation oven (UFP 600, Memmert, Schwabach, Germany) at 58 °C for the whole period (90 days), and periodic monitoring of the samples was performed manually at 7, 14, 21, 28, and 90 days.

Water Vapor Permeability: The water vapor permeability was determined for MR, G-SMS, E-SMS, and PLA sheets using a dynamic vapor sorption (DVS intrinsic, Surface Measurement Systems, London, UK) instrument equipped with a Payne diffusion cell. The Payne cell was filled with silica gel, which was previously dried at 120 °C overnight. Samples were cut into round shapes slightly larger than the opening area of the Payne cell. The change in mass of the silica gel at 0, 50, 90, 50, and 0% RH was measured at 25 °C. The moisture vapor transmission rate *MVTR* was calculated from the slope of the moisture uptake by the drying agent Δm in a unit time Δt in Equation 3, and the water vapor permeability was determined considering the area of the cell opening (15.54 mm^2). At 50 and 90% RH (absorption), three different locations at each slope were used for the calculation of the average water vapor permeability.

$$MVTR = \frac{\Delta m}{\Delta t} \tag{3}$$

Density and Porosity: The envelope density ρ_e, including open and closed pores within the MR -, SMS -, and PLA sheets was calculated using Equation 4.

$$\rho_e = \frac{m}{Ad} \tag{4}$$

where m is the mass of specimens, A the area, and d is the thickness, while ρ_e of the foams was measured using an envelope density analyzer (GeoPyc 1360, Micromeritics GmbH, Unterschleißheim, Germany). Five foams with dimensions of ≈ 0.5 × 0.5 × 0.5 cm^3 were measured.

The skeletal density ρ_s was measured by Helium displacement pycnometer (AccuPyc, II 1340, Micromeritics GmbH, Unterschleißheim, Germany). A chamber of 1 cm^3 was used and 10 purges per measurement were applied. The sheets and foams were cut into pieces and dried overnight at 80 °C prior to measurements. 3–4 replicates of each material were measured and the average presented. Equation 5 was used to calculate the porosity ϕ of materials using ρ_e and ρ_s.

$$\phi = \left(1 - \frac{\rho_e}{\rho_s}\right) \times 100 \tag{5}$$

Specific Surface Area (SSA): The Brunauer-Emmett-Teller (BET) surface area for SMS foams was determined by N_2 physisorption (Micromeritics Gemini VII 2390a, Chemical Instruments AB, Stockholm, Sweden). The foams were first degassed at 115 °C for 4 h, followed by N_2 adsorption with relative vapor pressure of 0.01–0.3 at −196 °C.

Sorption Capacity of Water and Oil: SMS foams were immersed into distilled water, and mineral oil, respectively, for 5 min at room temperature. Excess water/oil on the bottom was removed with filter paper prior to weighing the foams. The measurement was performed in triplicates. The sorption capacity (*C*) was calculated by the following Equation 6:

$$C = \frac{M_s - M_0}{M_0} \tag{6}$$

where M_0 and M_s are the weights of the foam before and after immersion, respectively.

Stereomicroscopy: The surface of the sheets prepared from G-SMS and E-SMS was analyzed using a NIKON SMZ1270 stereomicroscope (BergmanLabora, Danderyd, Sweden) equipped with imaging software NIS-Elements D 4.30. All samples were investigated at a 0.75 times magnification.

Oxygen Permeability: G-SMS and PLA sheets (25 mm in diameter and thickness d of 100 ± 10 µm and 110 ± 15 µm, respectively) were placed on α-alumina supports (Fraunhofer IKTS, Germany) and clamped between two O-rings in the inlet tube and the outlet tube was connected to a graduated pipette containing soap water when gas flows, it forms bubbles traveling through the pipette. A constant gas pressure p_1 of 1 and 5 bar

was applied to the inlet. The steady-state gas flow rate J_{st} can be calculated by the distance bubbles traveling through a given volume per time at 24 °C, 53% RH. The permeability coefficient P can be calculated using Equation 7.

$$P = \frac{J_{st}\, d}{p_1} \tag{7}$$

3 samples of each material were tested.

Supporting Information

Supporting Information is available from the Wiley Online Library or from the author.

Acknowledgements

The authors would like to thank Prof. Eero Kontturi at Aalto University, Finland for the carbohydrate analysis, Ing. Wolfgang Schlager from the Institute of Environmental Biotechnology at BOKU University for laser-cutting cosmetic masks, and Ass.-Prof. Mag. Dr. Hanspeter Kählig of the NMR Centre of the University of Vienna for the ssNMR measurements as well as Mag. Johannes Theiner from the laboratory of microanalytical services for the elemental analysis and Dr. Ossi Laitinen at Oulu University, Finland for the fiber size analysis. The authors are thankful for financial support from Bio4Energy strategic funding, Knut and Alice Wallenberg Foundation for WWSC, WISE programs, Treesearch, and the University of Vienna. Special thanks to Dr. Kathrin Weiland of Delft University of Technology, Netherlands, and the students at the Institute of Materials Chemistry and Research for contributing to the development of fungal-based sheet masks: Loïck Belvindrah (IMT Mines Ales), Fabian Edlinger and Markus Paunger at the University of Vienna, and project student Jessy Gindt at Luleå University of Technology working and SMS sorbents.

Conflict of Interest

The authors declare no conflict of interest.

Data Availability Statement

The data that support the findings of this study are available from the corresponding author upon reasonable request.

Keywords

mechanical properties, microstructure, mushroom residue, naturally bioactive, spent mushroom substrates

Received: July 17, 2024
Revised: August 31, 2024
Published online: September 27, 2024

[1] U. N. Faostat, https://data.un.org/Data.aspx?d=FAO&f=itemCode:449 (accessed: August 2024).
[2] Grand View Research, Inc., https://www.grandviewresearch.com/industry-analysis/mushroom-market (accessed: August 2024).
[3] U. Singh, P. Tiwari, S. Kelkar, D. Kaul, A. Tiwari, M. Kapri, S. Sharma, *eFood* **2023**, *4*, 122.
[4] M. K. Awasthi, V. Kumar, C. Hellwig, R. Wikandari, S. Harirchi, T. Sar, S. Wainaina, R. Sindhu, P. Binod, Z. Zhang, M. J. Taherzadeh, *Food Res. Int.* **2023**, *164*, 112318.
[5] K. Papoutsis, S. Grasso, A. Menon, N. P. Brunton, J. G. Lyng, J. C. Jacquier, D. J. Bhuyan, *Trends Food Sci. Technol.* **2020**, *99*, 351.
[6] W. T. Chou, I. C. Sheih, T. J. Fang, *J. Food Sci.* **2013**, *78*, 1041.
[7] B. C. Williams, J. T. Mcmullan, S. Mccahey, *Bioresour. Technol.* **2001**, *79*, 227.
[8] A. Gandia, J. G. van den Brandhof, F. V. W. Appels, M. P. Jones, *Trends Biotechnol.* **2021**, *39*, 1321.
[9] W. M. F. W. Nawawi, K. Y. Lee, E. Kontturi, A. Bismarck, A. Mautner, *Int. J. Biol. Macromol.* **2020**, *148*, 677.
[10] J. Janesch, M. Jones, M. Bacher, E. Kontturi, A. Bismarck, A. Mautner, *React. Funct. Polym.* **2020**, *146*, 104428.
[11] X. Fu, S. Zhang, X. Zhang, Y. Zhang, B. Li, K. Jin, X. Feng, J. Hong, X. Huang, H. Cao, Q. Yuan, P. Ai, H. Yu, Q. Li, *Adv. Funct. Mater.* **2023**, *33*, 2212570.
[12] E. Elsacker, M. Zhang, M. Dade-Robertson, *Adv. Funct. Mater.* **2023**, *33*, 2301875.
[13] J. Guo, M. Zhang, Z. Fang, *J. Sci. Food Agric.* **2022**, *102*, 5593.
[14] M. Xu, Y. Huang, R. Chen, Q. Huang, Y. Yang, L. Zhong, J. Ren, X. Wang, *Adv. Compos. Hybrid Mater.* **2021**, *4*, 1270.
[15] P. R. Lu, J. L. Xia, X. L. Dong, *ACS Sustainable Chem. Eng.* **2019**, *7*, 14841.
[16] M. Rinaudo, *Progress Polymer. Sci.* **2006**, *31*, 603.
[17] D. J. G. H. Wessels, *J. Gen. Microbiol.* **1979**, *114*, 99.
[18] W. M. F. W. Nawawi, K.-Y. Lee, E. Kontturi, R. J. Murphy, A. Bismarck, *ACS Sustainable Chem. Eng.* **2019**, *7*, 6492.
[19] W. M. F. W. Nawawi, M. P. Jones, E. Kontturi, A. Mautner, A. Bismarck, *Compos. Sci. Technol.* **2020**, *198*, 108327.
[20] C. Bilbao-Sainz, B. Sen Chiou, T. Williams, D. Wood, W. X. Du, I. Sedej, Z. Ban, V. Rodov, E. Poverenov, Y. Vinokur, T. McHugh, *Carbohydr. Polym.* **2017**, *167*, 97.
[21] C. Sun, P. Yue, R. Chen, S. Wu, Q. Ye, Y. Weng, H. Liu, Y. Fang, *Carbohydr. Polym.* **2022**, *291*, 119553.
[22] M. Latif, H. Khalid, N. Salman, F. Ahmed, *J. Appl. Emerging Sci.* **2022**, *12*, 27.
[23] P. Morganti, M. Coltelli, S. Danti, *Global J. Nanomedicine* **2018**, *3*, 1.
[24] P. Morganti, G. Morganti, H.-D. Chen, *J. Clinical Cosmetic Dermatology* **2019**, *3*, 1.
[25] P. Morganti, V. E. Yudin, G. Morganti, M. B. Colte, *Cosmetics* **2020**, *7*, 68.
[26] J. Harmon, *J. Textile Sci. Fashion Technol.* **2020**, *5*, 1.
[27] S. Gautier, E. Xhauflaire-Uhoda, P. Gonry, G. E. Piérard, *Int. J. Cosmet. Sci.* **2008**, *30*, 459.
[28] K. D. Hyde, A. H. Bahkali, M. A. Moslem, *Fungal Divers* **2010**, *43*, 1.
[29] D. Sivakumar, G. Bozzo, *Sustainability* **2023**, *15*, 11961.
[30] P. Morganti, G. Morganti, M. B. Coltelli, *Cosmetics* **2023**, *10*, 42.
[31] A. M. Abdel-Mohsen, J. Jancar, D. Massoud, Z. Fohlerova, H. Elhadidy, Z. Spotz, A. Hebeish, *Int. J. Pharm.* **2016**, *510*, 86.
[32] S. Xiong, C. Martín, L. Eilertsen, M. Wei, O. Myronycheva, S. H. Larsson, T. A. Lestander, L. Atterhem, L. J. Jönsson, *Bioresour. Technol.* **2019**, *274*, 65.
[33] F. Chen, S. Xiong, M. Latha Gandla, S. Stagge, C. Martín, *Bioresour. Technol.* **2022**, *347*, 126381.
[34] B. B. Ré, W. G. V. Junior, R. B. Postiguel, L. S. da Alves, C. E. C. Caitano, M. A. S. da Freitas, D. C. Zied, *Sci. Total Environ.* **2024**, *944*, 173976.
[35] H. Li, S. Yoshida, N. Mitani, M. Egusa, M. Takagi, H. Izawa, T. Matsumoto, H. Kaminaka, S. Ifuku, *Carbohydr. Polym.* **2022**, *284*, 119233.
[36] F. H. Mohd Hanafi, S. Rezania, S. Mat Taib, M. F. Md Din, M. Yamauchi, M. Sakamoto, H. Hara, J. Park, S. S. Ebrahimi, *J. Mater. Cycles Waste Manage.* **2018**, *20*, 1383.

[37] G. A. Holt, G. McIntyre, D. Flagg, E. Bayer, J. D. Wanjura, M. G. Pelletier, *J. Biobased Mater. Bioenergy* **2012**, *6*, 431.
[38] S. Manan, M. W. Ullah, M. Ul-Islam, O. M. Atta, G. Yang, *J. Bioresour. Bioprod.* **2021**, *6*, 1.
[39] M. Jones, A. Mautner, S. Luenco, A. Bismarck, S. John, *Mater. Des.* **2020**, *187*, 108397.
[40] GROWN bio, https://www.grown.bio/ (accessed: August 2024).
[41] N. Attias, M. Reid, S. C. Mijowska, I. Dobryden, M. Isaksson, B. Pokroy, Y. J. Grobman, T. Abitbol, *Adv. Sustain. Syst.* **2021**, *5*, 2000196.
[42] N. Konno, M. Kimura, R. Okuzawa, Y. Nakamura, M. Ike, N. Hayashi, A. Obara, Y. Sakamoto, N. Habu, *Wood Preserv.* **2016**, *42*, 157.
[43] W. Suksai, C. Chuensangjun, J. Wongsa, V. Rungsardthong, S. Vatanyoopaisarn, B. Thumthanaruk, R. Yeetsorn, B. P. Lamsal, in Proc. 2021*E3S Web Conf*, EDP Sciences, Les Ulis, France **2021**, https://doi.org/10.1051/e3sconf/202130202016.
[44] G. O. Michalenko, H. R. Hohl, D. Rast, *J. Gen. Microbiol.* **1976**, *92*, 251.
[45] B. Muszyńska, K. Kała, J. Rojowski, A. Grzywacz, W. Opoka, *Pol. J. Food Nutr. Sci.* **2017**, *67*, 173.
[46] N. Yousefi, M. Jones, A. Bismarck, A. Mautner, *Carbohydr. Polym.* **2021**, *253*, 117273.
[47] X. Kang, A. Kirui, A. Muszyński, M. C. D. Widanage, A. Chen, P. Azadi, P. Wang, F. Mentink-Vigier, T. Wang, *Nat. Commun.* **2018**, *9*, 2747.
[48] R. H. Newman, *Cellulose* **2004**, *11*, 45.
[49] Y. Ono, M. Takeuchi, A. Isogai, *Cellulose* **2022**, *29*, 2119.
[50] M. A. Nilforoushzadeh, M. A. Amirkhani, P. Zarrintaj, A. Salehi Moghaddam, T. Mehrabi, S. Alavi, M. M. Sisakht, *J. Cosmet. Dermatol.* **2018**, *17*, 693.
[51] X. Fan, X. Bai, L. Tan, C. Fang, X. Shen, H. Xu, Y. Wang, Y. Ma, Y. Li, X. Song, J. Hu, Y. Lu, X. Wei, J. Zhang, F. Li, Z. Zhu, S. Duan, Y. Zhou, H. Wu, W. Liu, *Macromol. Rapid Commun.* **2023**, *44*, 2300180.
[52] F. V. W. Appels, J. G. van den Brandhof, J. Dijksterhuis, G. W. de Kort, H. A. B. Wösten, *Commun. Biol.* **2020**, *3*, 334.
[53] P. C. Srinivasa, M. N. Ramesh, R. N. Tharanathan, *Food Hydrocolloids* **2007**, *21*, 1113.
[54] M. Österberg, J. Vartiainen, J. Lucenius, U. Hippi, J. Seppälä, R. Serimaa, J. Laine, *ACS Appl. Mater. Interfaces* **2013**, *5*, 4640.
[55] A. H. Bedane, M. Eić, M. Farmahini-Farahani, H. Xiao, *J. Memb. Sci.* **2015**, *493*, 46.
[56] J. L. Wiles, P. J. Vergano, F. H. Barron, J. M. Bunn, R. F. Testin, *J. Food Sci.* **2000**, *65*, 1175.
[57] J. G. H. Wessels, O. M. H. De Vries, S. A. Ásgeirsdóttir, F. H. J. Schuren, *Plant Cell* **1991**, *3*, 793.
[58] O. M. H. De Vries, M. P. Fekkes, H. A. B. Wiisten, J. G. H. Wessels, *Arch. Microbiol.* **1993**, *159*, 330.
[59] L. G. Greca, A. Azpiazu, G. Reyes, O. J. Rojas, B. L. Tardy, E. Lizundia, *Carbohydr. Polym.* **2024**, *325*, 121561.
[60] L. Winandy, F. Hilpert, O. Schlebusch, R. Fischer, *Sci. Rep.* **2018**, *8*, 12033.
[61] L. Berglund, I. Anugwom, M. Hedenström, Y. Aitomäki, J. P. Mikkola, K. Oksman, *Cellulose* **2017**, *24*, 3265.
[62] B. D. James, C. P. Ward, M. E. Hahn, S. J. Thorpe, C. M. Reddy, *ACS Sustainable Chem. Eng.* **2024**, *12*, 1185.
[63] G. X. Wang, D. Huang, J. H. Ji, C. Völker, F. R. Wurm, *Adv. Sci.* **2021**, *8*, 2001121.
[64] L. Berglund, F. Forsberg, M. Jonoobi, K. Oksman, *RSC Adv.* **2018**, *8*, 38219.
[65] M. G. Hoskin, A. J. Underwood, P. Archambault, Properties of naturally-degrading sorbents for potential use in the clean-up of oil-spills in sensitive and remote coastal habitats, Centre for Research on Ecological impact on costal cities. Marine ecology laboratories (ALL) University of Sydney NSW, **2006**.
[66] B. Doshi, M. Sillanpää, S. Kalliola, *Water Res.* **2018**, *135*, 262.
[67] M.-B. Wu, S. Huang, T.-Y. Liu, J. Wu, S. Agarwal, A. Greiner, Z.-K. Xu, *Adv. Funct. Mater.* **2021**, *31*, 2006806.
[68] C. Xu, S. Guan, J. Xu, W. Gong, T. Liu, X. Ma, C. Sun, *Carbohydr. Polym.* **2021**, *252*, 117210.
[69] M. P. Arrieta, J. López, E. Rayón, A. Jiménez, *Polym. Degrad. Stab.* **2014**, *108*, 307.